Light-Driven Spiral Deformation of Supramolecular Helical Microfibers by Localized Photoisomerization

Deng, Yuanxin; Zhang, Qi; Nie, Ting; Xu, Fan; Costil, Romain; Gong, Xue Qing; Tian, He; Feringa, Ben L.; Qu, Da Hui

Published in:
Advanced optical materials

DOI:
10.1002/adom.202101267

ADVANCED OPTICAL MATERIALS
www.advopticalmat.de

Light-Driven Spiral Deformation of Supramolecular Helical Microfibers by Localized Photoisomerization

Yuanxin Deng, Qi Zhang, Ting Nie, Fan Xu, Romain Costil, Xue-Qing Gong, He Tian, Ben L. Feringa, and Da-Hui Qu**

Stimuli-responsive mechanical deformations widely occur in biological systems but the design of biomimetic shape-changing materials, especially those based on noncovalent interactions, remains highly challenging. Here, hydrogen-bonded supramolecular microfibers are reported, which can perform light-driven spiral deformation by switching an intrinsic azobenzene unit without monomer dissociation. The key design feature rests on rationally spaced multiple hydrogen bonds, which inhibits the disassembly pathway upon irradiation, allowing partial photomechanical actuation of the azobenzene cores in the confined environment of the assemblies. The light-controlled deformation process of the supramolecular microfibers can be switched in a fully reversible manner. This combination of confinement-inhibited disassembly and photoswitching to induce assembly deformation and actuation along length scales supports a distinctive strategy to design supramolecular materials with photomechanical motion.

1. Introduction

Responsiveness at all length scales is a key feature of living systems and the essential mechanism to enable mechanical motion.[1] One of the main challenges is how to mimic life-like responsive behavior in molecular systems using synthetic molecular machines to design soft actuators and biomimetic smart materials.[2] The progress in supramolecular chemistry enables the fabrication of complex architectures with unique dynamic functions in various hierarchical assemblies and at distinct length and time scales.[3] Supramolecular polymers, formed by noncovalent self-assembly of small molecules, are particularly attractive as they exhibit intrinsically dynamic functions,[4] including reversibility,[5] adaptiveness,[6] and self-repair properties.[7] The stimuli-responsive ability of supramolecular polymers has been explored by introducing artificial molecular switches and machines.[8] For example, these polymers can respond to light stimuli by the introduction of photochromic molecules, such as azobenzenes, diarylethenes, spiropyrans, and their derivatives.[9] The unique advantage of light stimuli is that it enables supramolecular materials[10] to be manipulated in a remote and instant mode, exhibiting great potential in applications toward soft actuators,[11] artificial muscles,[12] and light-healing coatings.[5e]

A key question is how to amplify the molecular-level photoactuation from nano to macroscopic dimensions to achieve global responsiveness of the supramolecular architectures.[1,2,12,13] However, the realization of this delicate interplay of dynamic functions remains very challenging because of the intrinsic reversibility of supramolecular systems, which usually leads to the photochemical lability disassembly of materials.[14] To enable photoactuation and meanwhile overcome the photodissociation process, it is crucial to stabilize the supramolecular architectures by engineering the binding affinity and hierarchy of multiple noncovalent interactions.[13d] Very recently, the Feringa group demonstrated the photochemically driven macroscopic actuation of nanofibers by cross-linking and stabilizing the primary supramolecular structures via strong metal carboxylate complexes.[12] The pathway of photoactuation without disassembly enabled the successful energy conversion from the absorbed light to mechanical work, exhibiting promising mechanical, i.e., muscle type and functions.

We present here a more general and direct strategy by introducing rationally spaced multiple hydrogen bonds (H-bonds) to enable photoinduced spiral deformation of supramolecular

Y. Deng, Q. Zhang, T. Nie, X.-Q. Gong, H. Tian, B. L. Feringa, D.-H. Qu
Key Laboratory for Advanced Materials and Joint International Research Laboratory of Precision Chemistry and Molecular Engineering
Feringa Nobel Prize Scientist Joint Research Center
Frontiers Science Center for Materiobiology and Dynamic Chemistry
Institute of Fine Chemicals
School of Chemistry and Molecular Engineering
East China University of Science and Technology
Shanghai 200237, China
E-mail: b.l.feringa@rug.nl; dahui_qu@ecust.edu.cn

Y. Deng, Q. Zhang, F. Xu, R. Costil, B. L. Feringa
Stratingh Institute for Chemistry and Zernike Institute for Advanced Materials
Faculty of Science and Engineering
University of Groningen
Nijenborgh 4, Groningen, AG 9747, Netherlands

The ORCID identification number(s) for the author(s) of this article can be found under https://doi.org/10.1002/adom.202101267.

DOI: 10.1002/adom.202101267

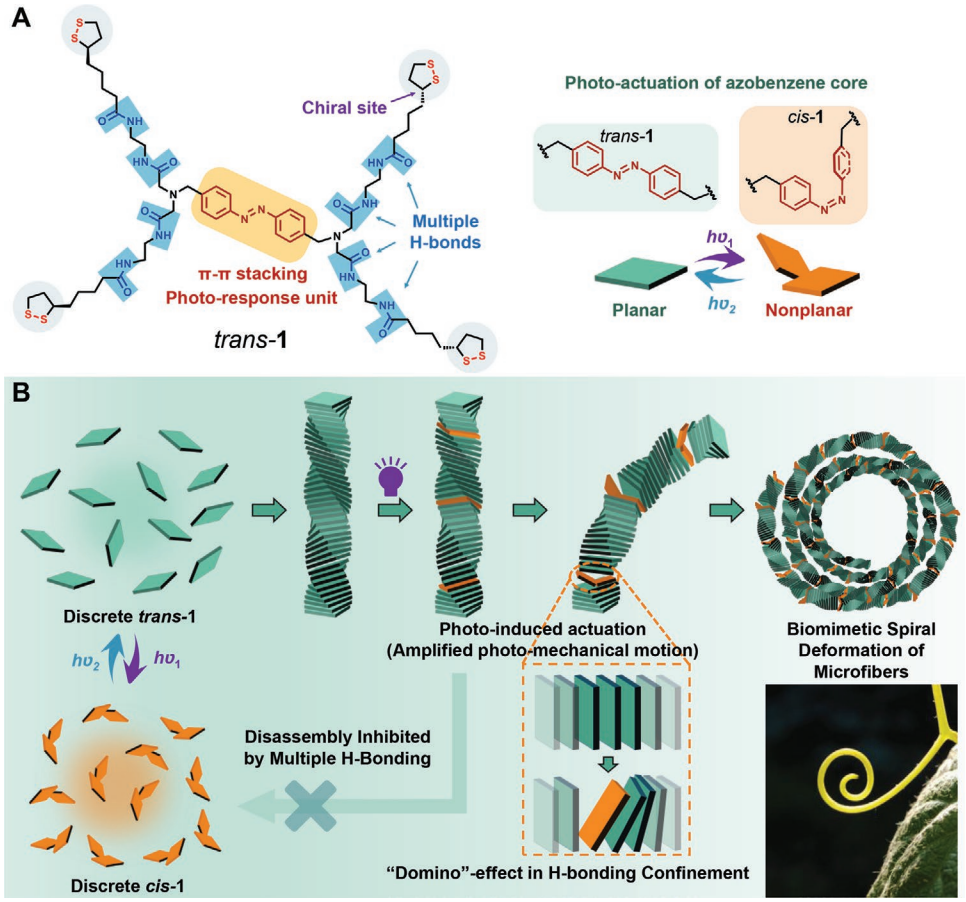

Figure 1. Structural design and schematic representation of the assembly of the photoresponsive building block. A) Molecular structure and photoisomerization of the *trans*-**1** and geometrical change leading to possible photomechanical actuation ($h\nu_1$ = 365 nm, $h\nu_2$ = 420 nm). B) Schematic representation of the light-induced deformation of the assemblies of *trans*-**1**. The supramolecular assembly of *trans*-**1** is initiated by lowering solvent polarity, leading to the formation of helical fibers, which can bend and spiral into coils upon irradiation of UV light (($h\nu_1$ = 365 nm, $h\nu_2$ = 420 nm). The inset image shows a typical spiral plant stem in Nature.

microfibers. The building block *trans*-**1** consists of a typical photoresponsive azobenzene core, eight amide bonds embedded in the side chains, and four terminal polymerizable 1,2-dithiolanes[15] functioning as homochiral entities and potential cross-linking units (**Figure 1**A). We anticipate that these structural features enable the stereo-controlled noncovalent self-assembly of the building blocks along the π–π stacking axial direction, forming helical supramolecular fibers with preferred handedness (Figure 1B). The azobenzene units confined in the high-density intermolecular H-bond system are mostly inhibited to induce motion upon photoisomerization. However, an important feature due to the supramolecular nature of the assembly is sufficient local flexibility to allow a very small portion of isomerized azobenzene units to be formed which can drive the global deformation of helical fibers to bend and spiral into spheres. The observed unique light-driven biomimetic spiraling motion is therefore attributed to the flexibility resulting from the rationally spaced H-bond arrays, enabling the in situ local photochemical actuation of azobenzene units in the fibers and amplification of the deformation through the supramolecular fibers.

2. Results and Discussion

Compound *trans*-**1** was prepared from 4,4′-bis(chloromethyl) azobenzene, Boc-protected 2,2′-azanediylbis(N-(2-aminoethyl) acetamide), and (+)-α-thioctic acid as outlined in Scheme S1 (Supporting Information). The detailed synthetic procedure for *trans*-**1** is provided in the Experimental Section (Supporting Information). The structure of *trans*-**1** was confirmed by ^{1}H NMR, ^{13}C NMR, and high-resolution mass analysis (HR-MS) (for details see Supporting Information).

The molecular structure of *trans*-**1** features a planar aromatic core with multiple amide groups, which is reminiscent of a typical discotic-like monomer structure[16] to form supramolecular assemblies by cooperative π–π stacking and H-bonds (**Figure 2**A). Compound *trans*-**1** exhibited good solubility in organic solvents such as dichloromethane (CH_2Cl_2), forming a yellow and transparent solution (Figure 2B). Dynamic light scattering (DLS) showed that the size distribution was mainly located at around 1 nm (the dimension of *trans*-**1**) (Figure 2C), indicating molecular dispersion of *trans*-**1** in CH_2Cl_2. The good solubility in apolar CH_2Cl_2 solution can be attributed

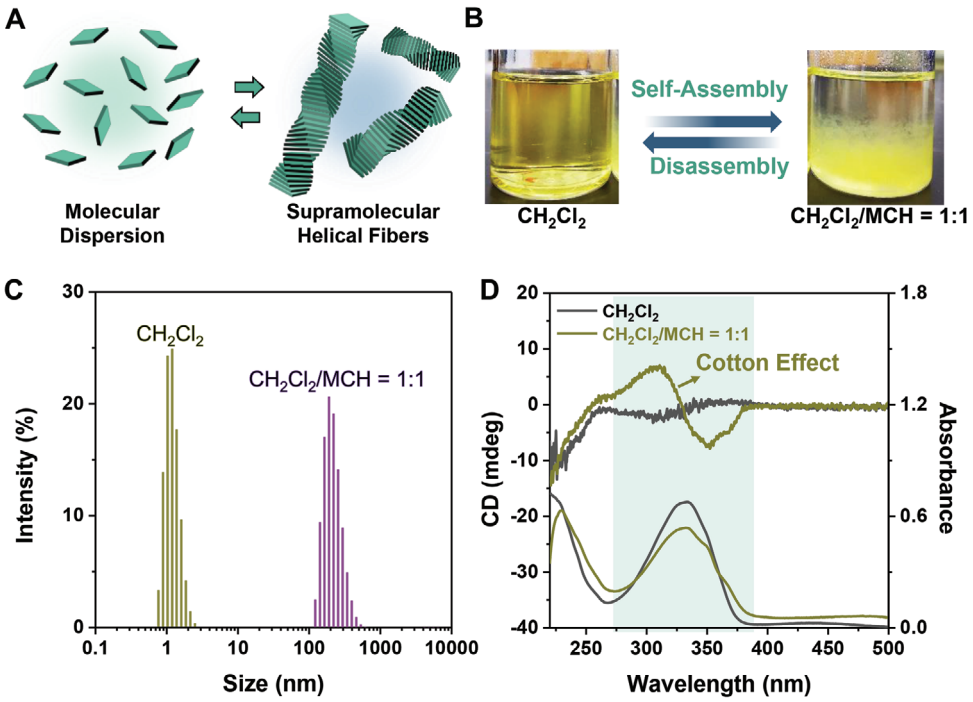

Figure 2. A) Schematic representation of the supramolecular helical self-assembly of building block *trans*-**1**. B) Photographs of the solutions of *trans*-**1** in CH_2Cl_2 and 1:1 mixed solution of CH_2Cl_2/MCH. C) Dynamic light scattering (DLS) size distribution of the solution of *trans*-**1** in CH_2Cl_2 (yellow bars), and 1:1 mixed solution of CH_2Cl_2/MCH (purple bars), respectively. D) UV-Vis absorption spectra and circular dichroism (CD) spectra of *trans*-**1** in CH_2Cl_2 ($c = 2 \times 10^{-4}$ M, $d = 1$ mm) and 1:1 mixed solution of CH_2Cl_2/MCH ($c = 2 \times 10^{-4}$ M, $d = 1$ mm).

to the alkyl chains and side-chain flexibility. The addition of 1 equiv. v/v of methylcyclohexane (MCH), a strongly H-bond-supporting solvent,[9f] into the CH_2Cl_2 solution of *trans*-**1** led to immediate aggregation, forming a turbid solution (Figure 2B). Yellow aggregates (100–400 nm in size) were formed after aging the turbid solution, and DLS confirmed the complete aggregation of *trans*-**1** even in a diluted solution (CH_2Cl_2/MCH = 1:1) (Figure 2C). X-ray diffraction (XRD) patterns indicated the amorphous nature of the microfibers and the existence of π–π stacking interactions (Figure S1, Supporting Information). Infrared (IR) spectra indicated complete hydrogen bonding of the amide bonds in the supramolecular assemblies of *trans*-**1** (Figure S2, Supporting Information).

UV-Vis absorption spectra showed a decreased intensity of the major absorption band (λ_m = 330 nm) of *trans*-**1** after aggregation (Figure 2D). The slightly increased absorption intensity in the visible-light region (400–500 nm) was due to the light scattering effect as a result of increased turbidity. Circular dichroism (CD) spectra showed a distinctive Cotton effect at the absorption region (280–400 nm) of the azobenzene chromophore in the aggregation state (Figure 2D and Figure S3, Supporting Information). The weak but detectable CD signal of *trans*-**1** in CH_2Cl_2 was attributed to the intrinsic chiral chromophore of 1,2-dithiolane unit. The observed strong Cotton effect of the solution of aggregated *trans*-**1** points to the existence of helical assembled structures of azobenzene core units.[17] Temperature-dependent CD spectra exhibited little changes from 263 to 313 K (Figure S4, Supporting Information), suggesting good thermal stability of the supramolecular helical assemblies owing to the multiple hydrogen bonds.

The photoresponsive nature of the azobenzene unit enabled bistable switching of *trans*-**1** in the solution phase. The typical π–π absorption band of *trans*-azobenzene disappeared upon irradiation with UV light (365 nm), and meanwhile the absorption of n–π band increased (**Figure 3**A). The clear isosbestic points at 393 and 283 nm indicate a selective photochemical isomerization of *trans*-**1** in CH_2Cl_2. The photostationary state of *trans*-**1** was obtained (*cis*-**1**/*trans*-**1** = 86/14) from time-resolved ^{1}H NMR spectra (Figures S5 and S6, Supporting Information), indicating the high isomerization efficiency of *trans*-**1** in solution. The excellent reversibility was confirmed by the real-time recorded UV-Vis absorption spectra of the CH_2Cl_2 solutions of *trans*-**1** during irradiation of 365 nm (Figure 3B and Figure S7, Supporting Information).

Next the morphologies of the aggregates of *trans*-**1** and *cis*-**1** were investigated by field emission scanning electron microscopy (FESEM) and transmission electron microscopy (TEM) (Figure 3D–F, and Figures S8 and S9, Supporting Information) as a function of isomers and solvents. The assemblies of *trans*-**1** were observed as helical microfibers with a high length-to-diameter ratio (Figure 3D). The statistic distribution showed a varying diameter ranging from 7 to 26 nm (Figure S10, Supporting Information). Interestingly, all the helical fibers were found as an *M*-type helix (Figure 3D), confirming the single handedness of the supramolecular assemblies. This uniformity indicated the effectiveness of chirality transfer from the central chirality of the 1,2-dithiolanes units to supramolecular chirality of the assembled fibers.

When 1 equiv. v/v of MCH was added to a mixture of *trans*-**1** and *cis*-**1** in CH_2Cl_2 solution obtained by the irradiation

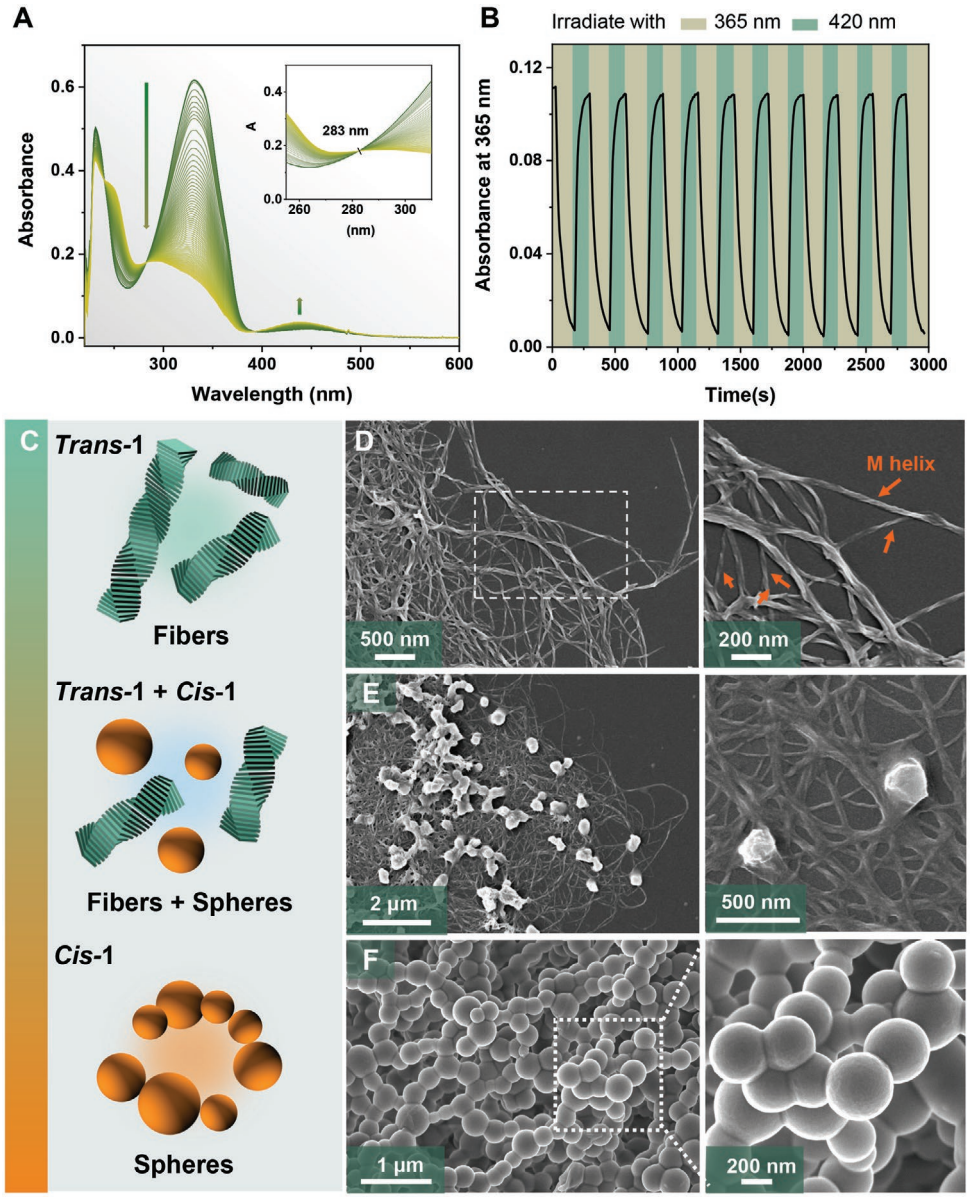

Figure 3. Photoswitching properties and aggregate morphologies of *trans*-**1** and *cis*-**1**. A) UV-Vis absorption spectra of *trans*-**1** in CH_2Cl_2 before and after irradiation of UV light (365 nm) ($c = 2 \times 10^{-5}$ M, $d = 1$ cm, CH_2Cl_2). B) Real-time detection of absorbance at 365 nm in multiple photoswitching cycles ($c = 1 \times 10^{-5}$ M, $d = 1$ cm, CH_2Cl_2). C) Schematic representation of the aggregates formed by *trans*-**1** and *cis*-**1** in the mixed solvents (CH_2Cl_2/MCH = 1:1). D–F) Representative field emission scanning electron microscopy (FESEM) images of the assemblies formed by *trans*-**1** (D), mixture of *trans*-**1** and *cis*-**1** (solution irradiated for 90 s) (E), and mixture at PSS (*cis*-**1**: *trans*-**1** = 86: 14) (F). The mixtures of *trans*-**1** and *cis*-**1** were obtained by irradiating the CH_2Cl_2 solution of *trans*-**1** with a given time and then the aggregation was induced by adding 1 equiv. v/v of MCH.

of UV light (365 nm, 90 s), the FESEM images showed the aggregates as mixture of helical fibers and spheres (Figure 3E, and Figure S11, Supporting Information). The helical fibers were consistent with those obtained by assembling pure *trans*-**1**, suggesting the homogeneity of the helical assemblies. Furthermore, the morphology of the resulting aggregates, with mainly *cis*-**1** present (86% at PSS state confirmed by ^{1}H NMR (Figure S5, Supporting Information)), was found to be spheres (Figure 3F, and S9, Supporting Information). CD measurement further confirmed the absence of chiral amplification in the aggregates of *cis*-**1** (Figure S12, Supporting Information). These observations indicated the remarkably difference in assembly between *trans*-**1** and *cis*-**1** which is attributed to the large change in geometry (planarity to nonplanarity) of the azobenzene cores. Further investigations by CD and UV-Vis spectroscopy proved that the *cis*-**1** aggregates can transform into *trans*-**1** helical assemblies upon visible-light irradiation (420 nm) or thermal isomerization in dark (Figures S13 and S15, Supporting Information). Thus, by orthogonalizing the reversible solvent-induced assembly/disassembly and light-controlled isomerization of monomers, the morphologies (and chirality) of supramolecular assemblies in this system can

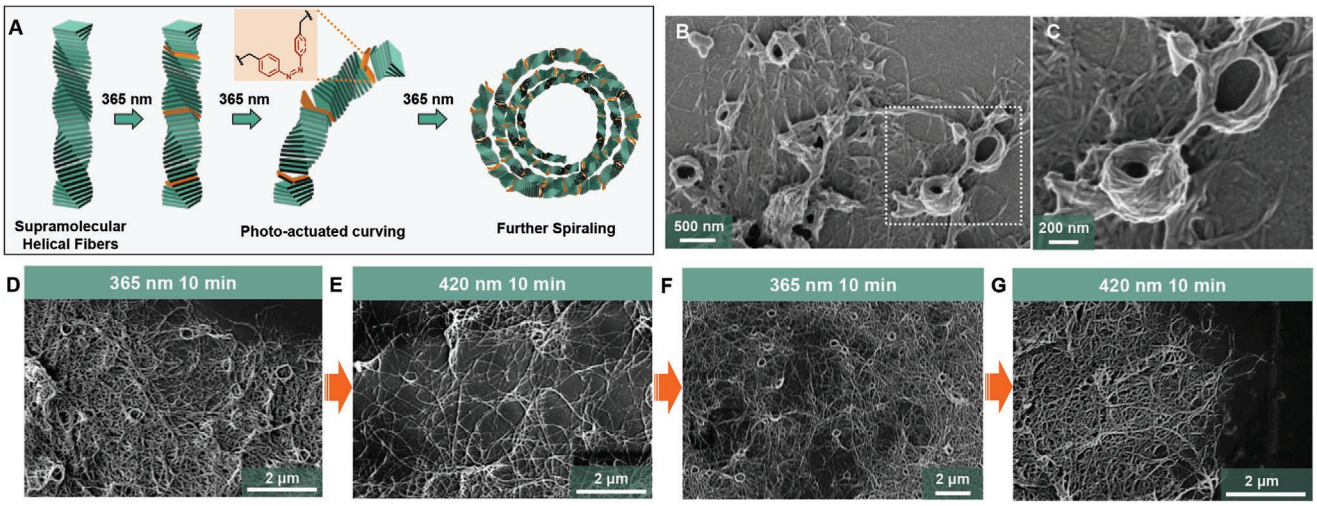

Figure 4. Photochemical-driven spiral deformation of supramolecular helical self-assembly of building block *trans*-**1**. A) Schematic representation of the light-induced spiral deformation process. B,C) Representative field emission scanning electron microscopy (FESEM) images of the spiral deformation of helical assemblies after UV irradiation (365 nm). D–G) Representative FESEM images of the reversible interconversion of the supramolecular microfibers from helical to spiral aggregates (and vice-) driven by irradiation with UV (365 nm) and visible (420 nm) light.

be dynamically modulated between chiral fibers and achiral spheres.

Having established the presence of remarkable difference in assembly behaviors between *trans*-**1** and *cis*-**1**, we further explored the important questions: Will the photoresponsive behavior of *trans*-**1** still be operating in the confined space of supramolecular helical assemblies? How is this "in situ" molecular isomerization affecting the global assemblies? Much to our surprise, we found a light-driven spiraling deformation in this system (**Figure 4**A,B). The supramolecular helical microfibers of *trans*-**1** were irradiated with UV light (365 nm) and FESEM analysis showed that many spiral microfibers were formed after UV irradiation (Figure 4B,C), while the helicity of the spiral fibers were preserved. UV-Vis absorption spectra showed a minimal decrease of the π–π^* absorption band after irradiation with light at 365 nm for 30 s (**Figure 5**A), indicating that only a very small number of azobenzene units undergo photoisomerization. Meanwhile, no significant change was observed after irradiation in the CD spectra (Figure 5A), providing further support for the chiral helical assemblies retaining after irradiation (365 nm). Moreover, most of the UV-light-induced spiral microfibers can recover back to the original state, i.e., helical microfiber, by irradiation with visible light (420 nm) (Figure 4D–G and Figure S16, Supporting Information) or aging in dark to allow thermal *cis-trans* isomerization (Figure S17, Supporting Information). Longer irradiation times, up to 30 min UV light, led to a higher spiral deformation ratio as well as some semi-spheres formed by the spiral fibers (Figure S18, Supporting Information).

To further understand the supramolecular self-assembly and photoactuation process, molecular dynamics (MD) simulations were performed (Figure 5B and Figures S19–S21, Supporting Information; Computational details are given in Supporting Information). Planar *trans*-**1** molecule can form multiple intermolecular H-bonds to produce supramolecular assemblies with a face-twisting-angle of 5° (Figures S19 and S20, Supporting Information). By replacing one of the assembled *trans*-**1** units by *cis*-**1**, MD simulation results showed that the presence of a single *cis*-**1** molecule leads to a local curvature (about 10°) of the axle direction of aggregated *trans*-**1** (Figure 5B). Therefore, it can be anticipated that this geometry-induced curvature might be the mechanism by which localized photoisomerization could be amplified into a global deformation of the supramolecular helical fibers.

The *cis*-**1** molecules confined in the H-bonding environment of supramolecular assemblies exhibited good reversibility over 10 cycles of photoisomerization by alternant irradiation with UV (365 nm) and visible light (420 nm) (Figure 5C). To further study how the supramolecular confinement affects the isomerization properties, we compared the half-life ($t_{1/2}$) of *cis*-**1** in different environments. Surprisingly, the half-life of *cis*-**1** in the assembled state was found to be much shorter than that in well-dispersed state (Figure 5D and Figure S22, Supporting Information). In principle, the decrease of solvent polarity should prolong the half-life of *cis*-azobenzenes.[18] Hence, the observed inverse effect on stability of *cis*-**1** suggests that the unique H-bonding environment accelerates the thermal reverse isomerization of *cis*-**1**. This might be attributed to a less stable strained nature of *cis*-**1** in the assemblies, decreasing the energy barrier between *trans*-**1** and *cis*-**1** and allowing a faster thermal reverse isomerization process.

Therefore, combining all the above data, the photoinduced deformation of helical microfibers of *trans*-**1** can be attributed to a photoactuation mechanism as indicated schematically in Figure 4A. The azobenzene units are confined in an anisotropic and single-handedness chiral space produced by the rationally positioned multiple H-bonds. The proper spatial distance in the H-bonding arrays provided sufficient flexibility to enable photoisomerization *trans* to *cis* of some of the assembled azobenzene units (Figure 5A). Intriguingly, the presence of these small amounts of isomerized azobenzene units do not seem to trigger the dissociation of supramolecular helical fibers, but instead are driving the global deformation of the fibers toward curved and spiraled spheres (Figure 4B–G). As a consequence,

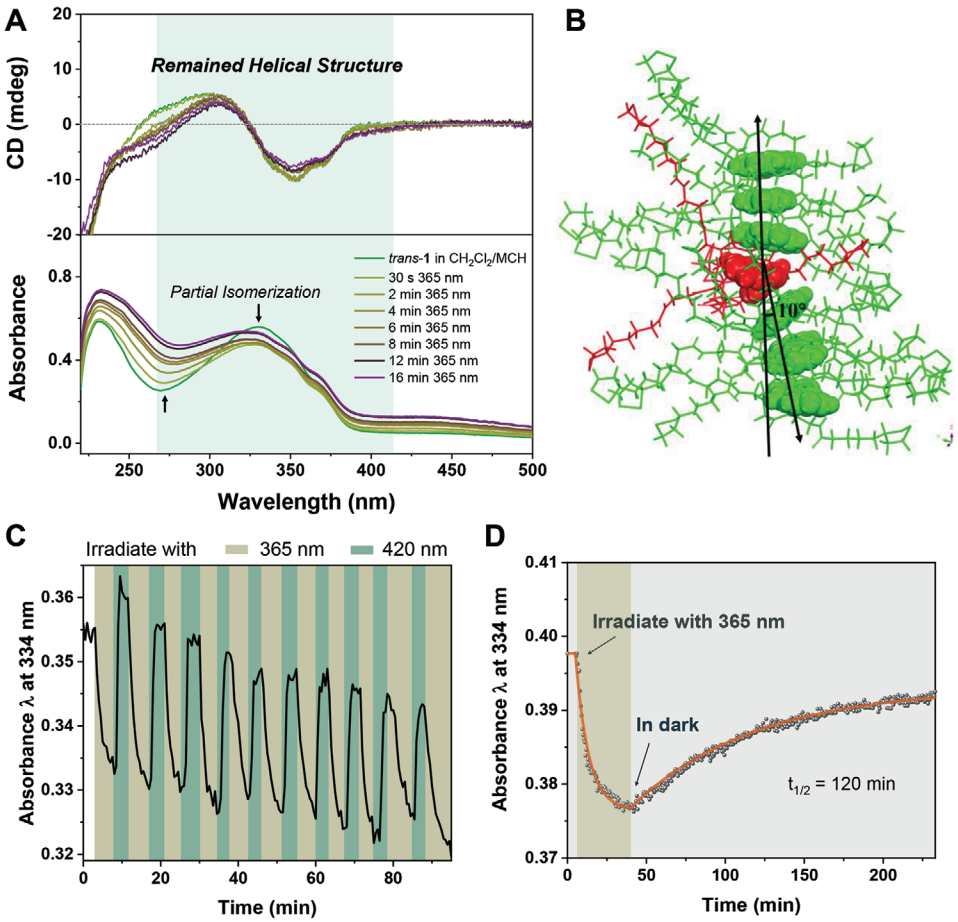

Figure 5. A) UV-Vis absorption spectra and circular dichroism (CD) spectra of the helical assemblies under UV light irradiation (λ = 365 nm, $c = 2 \times 10^{-4}$ M, d = 1 mm, CH_2Cl_2/MCH = 1:1). B) The calculated assembling model of six *trans*-**1** molecules (green) and one *cis*-**1** (red) molecule in equilibrium by molecular dynamic simulation at 10 ps. To illustrate the azobenzene cores clearly, these units are shown in CPK model. C) Real-time absorbance detection of the reversible photoswitching process of assembled *trans*-**1** (MCH/CH_2Cl_2 = 1:1, λ = 365 nm). D) For *cis*-**1** in the assembled system (MCH/CH_2Cl_2 = 1:1) a half-life ($t_{1/2}$ = 120 min) was determined, while the $t_{1/2}$ was 32.2 h under nonassembled condition (pure CH_2Cl_2) (Figure S22, Supporting Information).

the nanoscale molecular actuation of azobenzene units was delivered, transferred, and amplified along the supramolecular assembled backbone toward a larger mesoscopic scale spiral structure in a fully reversible manner.

3. Conclusion

In summary, we have demonstrated a supramolecular strategy to design photoresponsive supramolecular helical fibers, which, instead of disassembling by irradiation, could perform light-driven biomimetic spiral deformation. Importantly, this global deformation motion at the micrometer scale is driven by the localized isomerization of azobenzene units, amplifying the molecular motion toward the mesoscopic level. These findings indicate that multiple H-bonding interactions, one of the most typical noncovalent bonds in biological systems, in combination with photoswitches, can afford a robust supramolecular matrix still enabling intermolecular mechanical transmission and amplification, providing a noncovalent way to designing biomimetic responsive materials and soft actuators.

Supporting Information

Supporting Information is available from the Wiley Online Library or from the author.

Acknowledgements

This work was supported by National Natural Science Foundation of China (Grants 22025503, 21790361, 21871084, and 21672060), Shanghai Municipal Science and Technology Major Project (Grant 2018SHZDZX03), the Fundamental Research Funds for the Central Universities, the Program of Introducing Talents of Discipline to Universities (Grant B16017), Program of Shanghai Academic/Technology Research Leader (Grant 19XD1421100), and the Shanghai Science and Technology Committee (Grant 17520750100). B.L.F. acknowledges the financial support of the Netherlands Ministry of Education, Culture and Science (Gravitation program 024.601035). Y.D. acknowledges the financial support of China Scholarship Council. This project has received funding from the European Union's Horizon 2020 research and innovation programme under the Marie Skłodowska Curie grant agreement (Q.Z.: individual fellowship No. 101025041). The authors thank the Research Center of Analysis and Test of East China University of Science and Technology for help on the material characterization.

The authors also thank the Research Center of Analysis and Test of East China University of Science and Technology for help on the material characterization.

Conflict of Interest

The authors declare no conflict of interest.

Data Availability Statement

The data that support the findings of this study are available from the corresponding author upon reasonable request.

Keywords

photoresponsive materials, photoswitches, soft matter, supramolecular polymers, supramolecular self-assembly

Received: June 22, 2021
Revised: September 3, 2021
Published online: October 18, 2021

[1] a) J. M. Berg, J. L. Tymoczko, L. Stryer, *Biochemistry*, 5th ed., W.H. Freeman, New York **2002**; b) K. Kinbara, T. Aida, *Chem. Rev.* **2005**, *105*, 1377; c) C. J. Bruns, J. F. Stoddart, *The Nature of The Mechanical Bond: From Molecules to Machines*, John Wiley & Sons, Hoboken, NJ, USA **2016**; d) V. Balzani, M. Venturi, A. Credi, *Molecular Devices and Machines: A Journey into the Nanoworld*, **2006**, John Wiley & Sons, Hoboken, NJ, USA.

[2] a) A. Coskun, M. Banaszak, R. D. Astumian, J. F. Stoddart, B. A. Grzybowski, *Chem. Soc. Rev.* **2012**, *41*, 19; b) J. F. Lutz, J. M. Lehn, E. W. Meijer, K. Matyjaszewski, *Nat. Rev. Mater.* **2016**, *1*, 16024; c) J. P. Sauvage, *Angew. Chem., Int. Ed.* **2017**, *56*, 11080; d) J. F. Stoddart, *Angew. Chem., Int. Ed.* **2017**, *56*, 11094; e) B. L. Feringa, *Angew. Chem., Int. Ed.* **2017**, *56*, 11060; f) F. Lancia, A. Ryabchun, N. Katsonis, *Nat. Rev. Chem.* **2019**, *3*, 536; g) D. Dattler, G. Fuks, J. Heiser, E. Moulin, A. Perrot, X. Yao, N. Giuseppone, *Chem. Rev.* **2019**, *120*, 310; h) I. Aprahamian, *ACS Cent. Sci.* **2020**, *6*, 347; i) M. Baroncini, S. Silvi, A. Credi, *Chem. Rev.* **2020**, *120*, 200.

[3] a) J. M. Lehn, *Angew. Chem., Int. Ed.* **1988**, *27*, 89; b) J. M. Lehn, *Chem. Soc. Rev.* **2007**, *36*, 151; c) S. Erbas-Cakmak, D. A. Leigh, C. T. McTernan, A. L. Nussbaumer, *Chem. Rev.* **2015**, *115*, 10081; d) D. B. Amabilino, D. K. Smith, J. W. Steed, *Chem. Soc. Rev.* **2017**, *46*, 2404; e) I. V. Kolesnichenko, E. V. Anslyn, *Chem. Soc. Rev.* **2017**, *46*, 2385.

[4] a) L. Brunsveld, B. J. B. Folmer, E. W. Meijer, R. P. Sijbesma, *Chem. Rev.* **2001**, *101*, 4071; b) T. Aida, E. W. Meijer, S. I. Stupp, *Science* **2012**, *335*, 813; c) J. M. Lehn, *Prog. Polym. Sci.* **2005**, *30*, 814; d) L. Yang, X. Tan, Z. Wang, X. Zhang, *Chem. Rev.* **2015**, *115*, 7196; e) F. Huang, O. A. Scherman, *Chem. Soc. Rev.* **2012**, *41*, 5879.

[5] a) E. Krieg, H. Weissman, E. Shirman, B. Rybtchinski, *Nat. Nanotechnol.* **2011**, *6*, 141; b) T. T. Aida, E. W. Meijer, *Isr. J. Chem.* **2020**, *60*, 33; c) M. Saha, V. G. More, M. D. Aljabri, S. Chatterjee, M. Sahanawaz, S. Bandyopadhyay, S. V. Bhosale, *ACS Appl. Electron. Mater.* **2021**, *3*, 309; d) M. Samanta, A. Rananaware, D. N. Nadimetla, S. A. Rahaman, M. Saha, R. W. Jadhav, S. Bandyopadhyay, *Sci. Rep.* **2019**, *9*, 9670.

[6] a) B. Rybtchinski, *ACS Nano* **2011**, *5*, 6791; b) H. Shigemitsu, T. Fujisaku, W. Tanaka, R. Kubota, S. Minami, K. Urayama, I. Hamachi, *Nat. Nanotechnol.* **2018**, *13*, 165; c) M. Wehner, F. Würthner, *Nat. Rev. Chem.* **2020**, *4*, 38.

[7] a) P. Cordier, F. Tournilhac, C. Soulié-Ziakovic, L. Leibler, *Nature* **2008**, *451*, 977; b) D. W. Balkenende, C. A. Monnier, G. L. Fiore, C. Weder, *Nat. Commun.* **2016**, *7*, 10995; c) Y. Yanagisawa, Y. Nan, K. Okuro, T. Aida, *Science* **2018**, *359*, 72; d) Q. Zhang, C. Y. Shi, D. H. Qu, Y. T. Long, B. L. Feringa, H. Tian, *Sci. Adv.* **2018**, *4*, eaat8192; e) M. Burnworth, L. Tang, J. R. Kumpfer, A. J. Duncan, F. L. Beyer, G. L. Fiore, S. J. Rowan, C. Weder, *Nature* **2011**, *472*, 334.

[8] a) X. Yan, F. Wang, B. Zheng, F. Huang, *Chem. Soc. Rev.* **2012**, *41*, 6042; b) S. Ikejiri, Y. Takashima, M. Osaki, H. Yamaguchi, A. Harada, *J. Am. Chem. Soc.* **2018**, *140*, 17308; c) E. Weyandt, G. M. ter Huurne, G. Vantomme, A. J. Markvoort, A. R. Palmans, E. W. Meijer, *J. Am. Chem. Soc.* **2020**, *142*, 6295; d) T. S. MacDonald, B. L. Feringa, W. S. Price, S. J. Wezenberg, J. E. Beves, *J. Am. Chem. Soc.* **2020**, *142*, 20014.

[9] a) S. Yagai, A. Kitamura, *Chem. Soc. Rev.* **2008**, *37*, 1520; b) R. Klajn, *Chem. Soc. Rev.* **2014**, *43*, 148; c) Y. M. Zhang, N. Y. Zhang, K. Xiao, Q. Yu, Y. Liu, *Angew. Chem., Int. Ed.* **2018**, *57*, 8648; d) K. Yano, Y. Itoh, F. Araoka, G. Watanabe, T. Hikima, T. Aida, *Science* **2019**, *363*, 161; e) M. Yamauchi, T. Ohba, T. Karatsu, S. Yagai, *Nat. Commun.* **2015**, *6*, 8936; f) B. Adhikari, Y. Yamada, M. Yamauchi, K. Wakita, X. Lin, K. Aratsu, T. Ohba, T. Karatsu, M. J. Hollamby, N. Shimizu, H. Takagi, R. Haruki, S. Adachi, S. Yagai, *Nat. Commun.* **2017**, *8*, 15254; g) Y. Gu, E. A. Alt, H. Wang, X. Li, A. P. Willard, J. A. Johnson, *Nature* **2018**, *560*, 65; h) T. Dünnebacke, K. K. Kartha, J. M. Wiest, R. Q. Albuquerque, G. Fernández, *Chem. Sci.* **2020**, *11*, 10405.

[10] a) N. Roy, B. Bruchmann, J. M. Lehn, *Chem. Soc. Rev.* **2015**, *44*, 3786; b) E. Fuentes, M. Gerth, J. A. Berrocal, C. Matera, P. Gorostiza, I. K. Voets, S. Pujals, L. Albertazzi, *J. Am. Chem. Soc.* **2020**, *142*, 10069; c) A. Goulet-Hanssens, F. Eisenreich, S. Hecht, *Adv. Mater.* **2020**, *32*, 1905966; d) C. Kulkarni, R. H. N. Curvers, G. Vantomme, D. J. Broer, A. R. A. Palmans, S. C. J. Meskers, E. W. Meijer, *Adv. Mater.* **2021**, *33*, 2005720; e) S. Chen, R. Costil, F. K. C. Leung, B. L. Feringa, *Angew. Chem., Int. Ed.* **2021**, *60*, 11604.

[11] a) Y. Takashima, S. Hatanaka, M. Otsubo, M. Nakahata, T. Kakuta, A. Hashidzume, H. Yamaguchi, A. Harada, *Nat. Commun.* **2012**, *3*, 1270; b) J. Lee, S. Oh, J. Pyo, J. M. Kim, J. H. Je, *Nanoscale* **2015**, *7*, 6457; c) K. Iwaso, Y. Takashima, A. Harada, *Nat. Chem.* **2016**, *8*, 625; d) Q. Yu, X. Yang, Y. Chen, K. Yu, J. Gao, Z. Liu, P. Cheng, Z. Zhang, B. Agulia, S. Ma, *Angew. Chem., Int. Ed.* **2018**, *57*, 10192; e) E. Borré, J. F. Stumbé, S. Bellemin-Laponnaz, M. Mauro, *Angew. Chem., Int. Ed.* **2016**, *55*, 1313.

[12] a) J. Chen, F. K. C. Leung, M. C. Stuart, T. Kajitani, T. Fukushima, E. van der Giessen, B. L. Feringa, *Nat. Chem.* **2018**, *10*, 132; b) F. K. C. Leung, T. Kajitani, M. C. Stuart, T. Fukushima, B. L. Feringa, *Angew. Chem., Int. Ed.* **2019**, *58*, 10985; c) F. K. C. Leung, T. van den Enk, T. Kajitani, J. Chen, M. C. Stuart, J. Kuipers, T. Fukushima, B. L. Feringa, *J. Am. Chem. Soc.* **2018**, *140*, 17724.

[13] a) J. M. Abendroth, O. S. Bushuyev, P. S. Weiss, C. J. Barrett, *ACS Nano* **2015**, *9*, 7746; b) E. S. Epstein, L. Martinetti, R. H. Kollarigowda, O. Carey-De La Torre, J. S. Moore, R. H. Ewoldt, P. V. Braun, *J. Am. Chem. Soc.* **2019**, *141*, 3597; c) C. Li, A. Iscen, H. Sai, K. Sato, N. A. Sather, S. M. Chin, Z. Álvarez, L. C. Palmer, G. C. Schatz, S. I. Stupp, *Nat. Mater.* **2020**, *19*, 900; d) Q. Zhang, D. H. Qu, H. Tian, B. L. Feringa, *Matter* **2020**, *3*, 355; e) B. L. Feringa, *Adv. Mater.* **2020**, *32*, 1906416.

[14] a) X. Yan, J. F. Xu, T. R. Cook, F. Huang, Q. Z. Yang, C. H. Tung, P. J. Stang, *Proc. Natl. Acad. Sci. U. S. A.* **2013**, *111*, 8717; b) J. del Barrio, P. N. Horton, D. Lairez, G. O. Lloyd, C. Toprakcioglu, O. A. Scherman, *J. Am. Chem. Soc.* **2013**, *135*, 11760; c) J. F. Xu, Y. Z. Chen, D. Wu, L. Z. Wu, C. H. Tung, Q. Z. Yang, *Angew. Chem.*,

Int. Ed. **2013**, *52*, 9738; d) S. J. Wezenberg, C. M. Croisetu, M. C. Stuart, B. L. Feringa, *Chem. Sci.* **2016**, *7*, 4341.

[15] a) J. A. Barltrop, P. M. Hayes, M. Calvin, *J. Am. Chem. Soc.* **1954**, *76*, 4348; b) K. Endo, T. Yamanaka, *Macromolecules* **2006**, *39*, 4038; c) E. K. Bang, G. Gasparini, G. Molinard, A. Roux, N. Sakai, S. Matile, *J. Am. Chem. Soc.* **2013**, *135*, 2088; d) X. Zhang, R. M. Waymouth, *J. Am. Chem. Soc.* **2017**, *139*, 3822; e) Q. Zhang, Y. Deng, H. Luo, C. Y. Shi, G. M. Geise, B. L. Feringa, H. Tian, D.-H. Qu, *J. Am. Chem. Soc.* **2019**, *141*, 12804; f) Y. Liu, Y. Jia, Q. Wu, J. S. Moore, *J. Am. Chem. Soc.* **2019**, *141*, 17075; g) Y. Deng, Q. Zhang, B. L. Feringa, H. Tian, D. H. Qu, *Angew. Chem., Int. Ed.* **2020**, *59*, 5278.

[16] T. Wöhrle, I. Wurzbach, J. Kirres, A. Kostidou, N. Kapernaum, J. Litterscheidt, J. C. Haenle, P. Staffeld, A. Baro, F. Giesselmann, S. Laschat, *Chem. Rev.* **2016**, *116*, 1139.

[17] a) N. Sakai, P. Talukdar, S. Matile, *Chirality* **2006**, *18*, 91; b) N. Berova, L. Di Bari, G. Pescitelli, *Chem. Soc. Rev.* **2007**, *36*, 914; c) E. Yashima, N. Ousaka, D. Taura, K. Shimomura, T. Ikai, K. Maeda, *Chem. Rev.* **2016**, *116*, 13752.

[18] S. Francesca, E. M. Terentjev, *Macromolecules* **2008**, *41*, 981.